Journal of Alloys and Compounds 509 (2011) 7826–7832

Contents lists available at ScienceDirect

Journal of Alloys and Compounds

journal homepage: www.elsevier.com/locate/jallcom

The influence of chemical disorder enhancement on the martensitic transformation of the $Ni_{50}Mn_{36}Sn_{14}$ Heusler-type alloy

E.C. Passamani[a,*], V.P. Nascimento[a], C. Larica[a], A.Y. Takeuchi[a], A.L. Alves[b], J.R. Proveti[b], M.C. Pereira[c], J.D. Fabris[d]

[a] Departamento de Física, Universidade Federal do Espírito Santo, 29075-910 Vitória, ES, Brazil
[b] Departamento de Ciências Matemáticas e Naturais, Universidade Federal do Espírito Santo, 29932-540, São Mateus, ES, Brazil
[c] Instituto de Ciência e Tecnologia, Universidade Federal dos Vales do Jequitinhonha e Mucuri (UFVJM), 39803-371 Teófilo Otoni, Minas Gerais, Brazil
[d] Departamento de Química, UFVJM, 39100-000 Diamantina, Minas Gerais, Brazil

ARTICLE INFO

Article history:
Received 18 March 2011
Received in revised form 3 May 2011
Accepted 5 May 2011
Available online 12 May 2011

Keywords:
Mössbauer spectroscopy
Magnetic properties
Martensitic transformation
Heusler alloys

ABSTRACT

The effect of chemical disorder over the martensitic phase transformation of the $Ni_{50}Mn_{36}Sn_{14}$ Heusler-type alloy was systematically investigated by performing X-ray diffractometry (DRX), DC magnetization and ^{57}Fe-doping and ^{119}Sn-Mössbauer spectroscopy measurements. DRX patterns are characteristics of a $L2_1$-type chemically disordered structure, where the presence of this disorder was first evaluated by analyzing the relative intensity of the (1 1 1) DRX reflection, which varies in the case of Fe-doped and practically disappears for the milled samples. In consequence, the magnetic properties of Fe-doped well-milled samples related to the martensitic phase transformation change substantially. 300 K ^{57}Fe-Mössbauer spectroscopy data suggest that the changes in the magnetic properties related to the martensitic transformation are intrinsically correlated to the ferromagnetic and paramagnetic fractions, which are respectively associated with Fe atoms replacing Mn- and Sn-sites. In the case of milled samples, the drastic reduction of alloy magnetization was explained by the increase of the number of Mn atoms in the shell regions, which have a reduced magnetic moment comparatively to those in the grain cores. The magnetization change and the temperature transition in the martensitic transformation are governed by the grain core. The initial magnetic properties and martensitic transformation can be recovered by a subsequent annealing on the milled sample.

1. Introduction

X_2YZ full Heusler alloys have a body-centered cubic structure with a face-centered superlattice at room temperature, and may be thought as being formed by four interpenetrating face-centered cubic lattices A, B, C, and D, in which A and C are identical (typically $L2_1$-type structure) [1]. Generally, in the ordered X_2YZ Heusler alloys, the X atoms lie on lattices A and C, Y atoms on B and Z atoms on D (see $L2_1$-conventional cell in Fig. 1). The $L2_1$-type structure (*Fm*3*m*) is distinguishable either from the A2-type structure (*Im*3*m*) or from the B2-type structure (P*m*3*m*), in which lattices B and D are also identical, by reflections of odd superlattice Bragg peaks, if there is a sufficiently large difference in the scattering factors of the atoms on B and D. In addition, the A2-type structure does not show superlattice diffraction lines, e.g., the (2 0 0) Bragg peak.

Regarding the $Ni_{50}Mn_{25}Sn_{25}$ (or simply Ni_2MnSn) Heusler alloy, it has been reported that Mn atoms govern its magnetic properties, whereas Ni and Sn atoms are assumed to have small or negligible magnetic moments in their crystallographic sites [2–4]. No structure phase transition has been observed in a broad temperature range, from high (∼ 400 K) to low temperatures (∼ 4.2 K). However, changes in distances either between Mn–Mn or Mn-nearest neighbor species, caused by different conditions in sample preparation, can considerably modify the magnetic properties of that Heusler-type alloy. In addition, changes in the Mn chemical environment can be partially done by chemical substitution or out-of-stoichometric procedures where, for example, Mn-rich $Ni_{50}Mn_{50-x}Sn_x$ Heusler-type compounds can be formed [5,6]. It should be emphasized that these Mn-rich alloys have attracted special attention of researchers, essentially due to their intrinsic structural and magnetic properties found in experiments where the temperature is varied [5–26]. From the structural point of view, these alloys may exhibit a martensitic phase transformation (MPT) depending either on the Mn concentration or on the local chemical disorder between the constituents of B and D-lattices. In general,

* Corresponding author. Tel.: +55 27 3335 7809; fax: +55 27 3335 2823.
E-mail address: edson@cce.ufes.br (E.C. Passamani).

0925-8388/$ – see front matter © 2011 Elsevier B.V. All rights reserved.
doi:10.1016/j.jallcom.2011.05.018

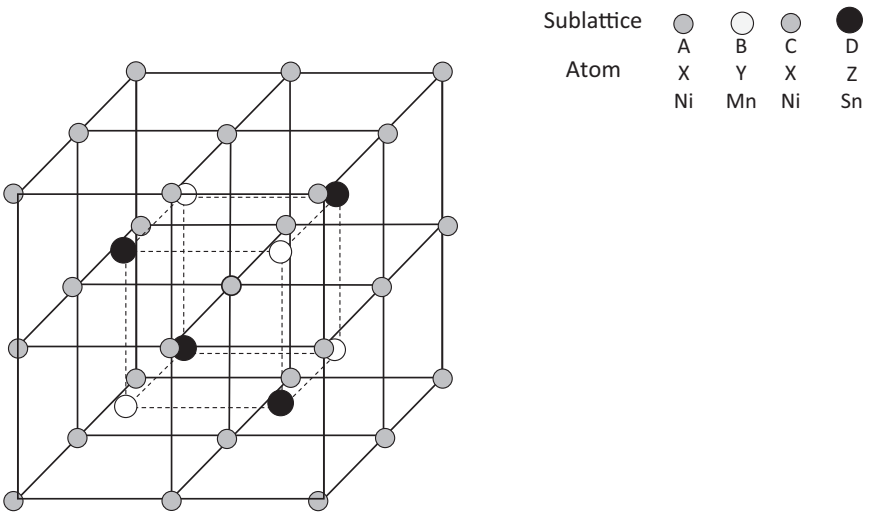

Fig. 1. Conventional cell for the X_2YZ full Heusler alloys.

this structural phase transformation seems to occur, in Mn-rich $Ni_{50}Mn_{50-x}Sn_x$ Heusler-type, from a highly symmetrical parent cubic phase ($Fm3m$) to a structure with lower symmetry ($Pmma$) [15].

Particularly, in the $Ni_{50}Mn_{36}Sn_{14}$ (or simply $Ni_2Mn_{1.44}Sn_{0.56}$) Heusler-type alloy, the martensitic transition temperature (T_M) value is about 220 K [15,20,21,23]. Above that, a ferromagnetic (FM) austenitic state is stable and the cubic crystal structure has a lattice parameter $a \approx 6$ Å [15]. Below T_M, in the martensitic phase, a FM orthorhombic four-layered structure is stabilized with a, b and c lattice parameters equal to 4.3 Å, 2.9 Å and 8.4 Å, respectively. On the other hand, due to the excess of Mn in the $Ni_{50}Mn_{36}Sn_{14}$, the crystal structure is not a pure $L2_1$-type structure found in the ordered $Ni_{50}Mn_{25}Sn_{25}$ ordinary Heusler compound. It is now a $L2_1$-B2-type disordered structure due to the extra Mn atoms occupying Sn-sites (D-lattices). Furthermore, while in the ordered $Ni_{50}Mn_{25}Sn_{25}$ compound the Mn atoms are ferromagnetically coupled, in the $Ni_{50}Mn_{36}Sn_{14}$ Heusler-type alloy, due the Mn excess, antiferromagnetic (AF) interactions also join to the ferromagnetic (FM) predominant phase, giving rise to the incipient AF compounds [5,6,24].

It has been reported that the partial substitution of Fe or Co in Ni or Mn sites results in a modification of T_M-values and the MPT disappears for large Fe doses [10,20]. This observation seems to be related to the chemical disorder effect (CDE), which causes changes in the Mn-neighborhood magnetic exchange interaction. Thus, the chemical disorder effect was studied by Fe-doping $Ni_{50}Mn_{36}Sn_{14}$ Heusler-type alloy with 1 at.% of ^{57}Fe tentatively occupying different sites of the $L2_1$-B2-type structure. It was also investigated the influence of milling on the magnetic properties of the iron-doped alloy samples.

^{57}Fe- and ^{119}Sn-Mössbauer spectroscopy measurements were performed in order to experimentally access the probe occupations in the lattice sites, as well as their chemical environments. These knowledge are essential to understand how magnetic properties are influenced by the new atomic arrangements modified by the chemical disorder of the $Ni_{50}Mn_{36}Sn_{14}$ Heusler-type alloy. These results will help to best comprehend the data from X-ray diffraction and magnetization measurements.

2. Experimental procedures

Fe-doped $Ni_{50}Mn_{36}Sn_{14}$-Heusler-type samples, namely $Ni_{50}Mn_{36}Sn_{14}$ (sample labeled 0% Fe), $Ni_{50}(^{57}Fe_{0.01}Mn_{0.99})_{36}Sn_{14}$ (1% ^{57}Fe–Mn), $(^{57}Fe_{0.01}Ni_{0.99})_{50}Mn_{36}Sn_{14}$ (1% ^{57}Fe–Ni) and $Ni_{50}Mn_{36}(^{57}Fe_{0.01}Sn_{0.99})_{14}$ (1% ^{57}Fe–Sn), were prepared in an arc-furnace from high graded chemicals of virtually pure Ni, Mn, Sn powder metals (better than 4N) and Fe metal isotopically 95%-enriched in ^{57}Fe. The main reason to use ^{57}Fe-rich instead of natural Fe is to trace and to get information about site occupation and local magnetism from ^{57}Fe placed in different sites of the $L2_1$-type structure using Mössbauer spectroscopy. The melted pellets were homogenized in a quartz evacuated tube at 1123 K for 48 h and after quenched in cold water (280 K). The powder samples used for X-ray analysis, Mössbauer spectroscopy and magnetization measurements were obtained by grinding pieces from the pellets, immersed in acetone, in an agate mortar. In addition, these alloys were also milled with a SPEX 8000 mill setup, for at maximum 4 min. The milling process has been done under argon atmosphere to prevent sample oxidation. More details of the milling tools and experimental procedures can be found in Ref. [27]. The milled samples were also annealed for 1 h at 1123 K and then they were characterized structurally and magnetically using the above experimental techniques.

Room temperature (RT; ~298 K) X-ray powder diffraction data were collected with a Rigaku diffractometer with Cu-Kα radiation (λ = 1.5418 Å). The powder samples were evenly homogenized in a sample holder, in a care to avoid eventual texture effect. A Shimadzu SSX 550 scanning electron microscope (SEM) was used to confirm the phase formation and its composition, using the energy dispersive X-ray spectroscopy (EDX), from polished flat pieces obtained from the central part of the annealed pellets. As we previously reported for other set of samples similarly prepared [20,21], more than 99% of the SEM image areas can be associated with a single phase corresponding to the $L2_1$-B2-type structure in accord with the X-ray diffraction result. These EDX results confirm that the nominal compositions indeed correspond to the planned alloys. No Fe signal from the EDX was detected, as its content lies below the experimental detection limit. Mössbauer experiments were carried out with a standard constant acceleration spectrometer, under transmission geometry. A ^{57}Co:Rh source with a nominal activity of about 30 mCi, and a $Ca^{119}SnO_3$ source with about 3 mCi, were respectively used to obtain the ^{57}Fe and ^{119}Sn Mössbauer spectra. The powder samples were sealed in a sample holder of the Mössbauer set-up for RT experiments. The ^{57}Fe spectra were obtained with 512 channels, whereas the ^{119}Sn spectra were taken with 1024 channels. The Mössbauer spectra were analyzed using NORMOS Program in the distribution version. In general, the spectra were fitted using two subspectra: a magnetic hyperfine field distribution (MHFD) and a paramagnetic component (singlet). The isomer shift (δ) values are given relative to metallic α-Fe obtained at RT for the case of ^{57}Fe and relatively to the $CaSnO_3$ source, for ^{119}Sn spectra. Field cooled (FC) and field heated (FH) magnetization versus temperature [$M(T)$] curves were recorded between 70 and 320 K using a commercial physical property measurement system (Quantum Design PPMS) coupled to an Evercool model cryostat and under an applied DC magnetic field up to 50 kOe. These curves were obtained using protocols described elsewhere [21]. As previously reported, any thermal hysteresis observed between FC and FH $M(T)$ curves can directly be associated with the first-order character of the martensitic phase transition (MPT).

3. Results and discussions

In Fig. 2(a), it is displayed the X-ray diffraction patterns for the three samples prepared with 1 at.% ^{57}Fe replacing one of the chemical constituents (Ni, Mn or Sn) of the $Ni_{50}Mn_{36}Sn_{14}$ Heusler-type alloy (1% ^{57}Fe–X, X = Ni, Mn and Sn). For comparison, two other X-ray patterns are also plotted: (i) for the Fe un-doped sample (0% Fe) and (ii) a computer-simulated diffractogram for the $L2_1$-type struc-

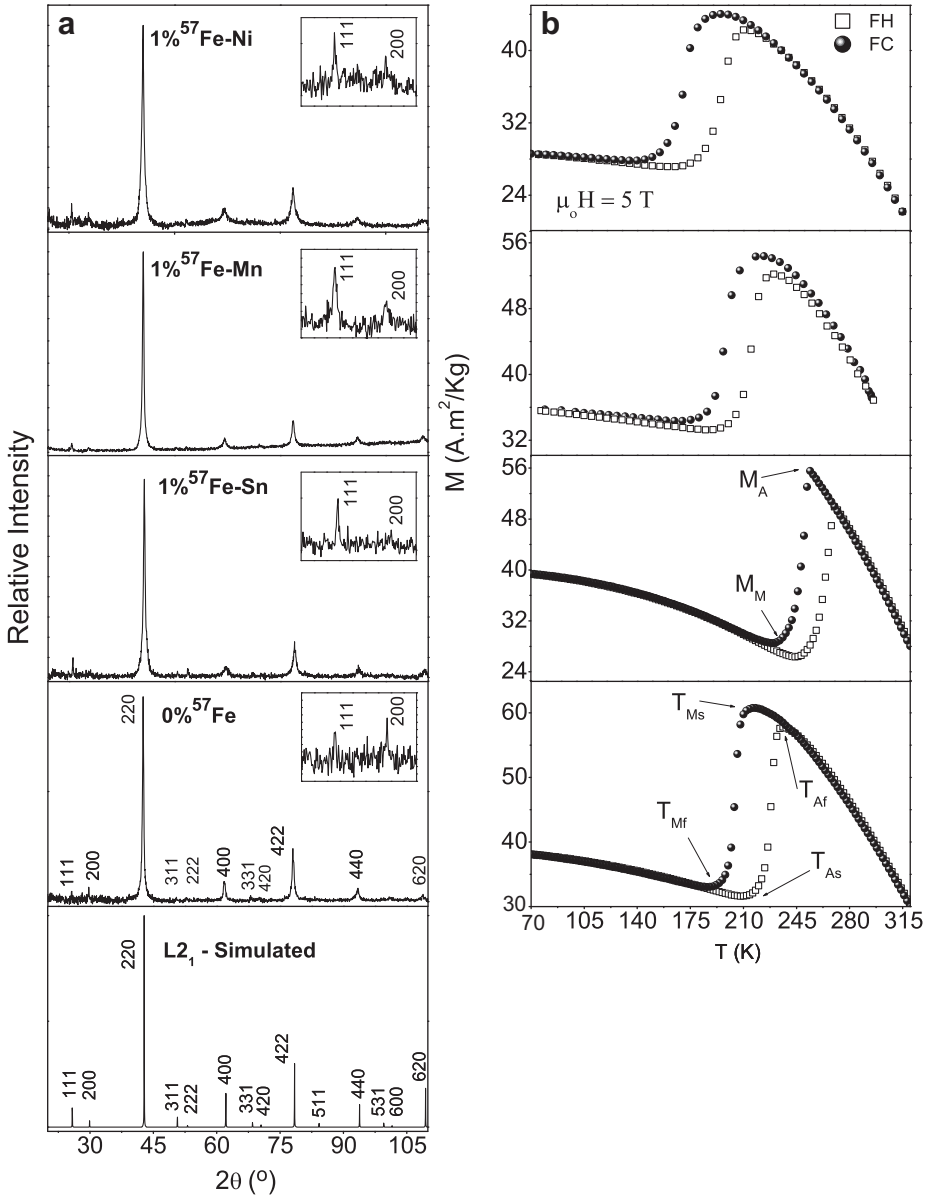

Fig. 2. (a) X-ray patterns of the Fe un-doped $Ni_{50}Mn_{36}Sn_{14}$ Heusler-type alloy (0% Fe) and the doped ones: 1% ^{57}Fe–Mn, 1% ^{57}Fe–Ni and 1% ^{57}Fe–Sn. A simulated pattern for the $L2_1$-type structure of the ordered Ni_2MnSn Heusler is also displayed. (b) $M(T)$ curves for the corresponding samples. These curves were recorded with a probe field of 50 kOe in FH and FC modes. The parameters are described in the text.

ture of the ordered $Ni_{50}Mn_{25}Sn_{25}$ Heusler alloy. Comparing these patterns, it is observed that all Bragg peaks found for the 1% ^{57}Fe-replacing samples match with the characteristic reflection lines of the $L2_1$-type simulated pattern. This observation indicates that the prepared samples do have $L2_1$-type structure, taking into account the fact that at least one of the odd reflection lines (fingerprints of the $L2_1$-type structure [1]) is present. However, it must be pointed out that two different features are observed for these Fe-doped samples: (i) the relative intensity of reflection (1 1 1) changes for the different samples, indicating an enhancement of chemical disorder caused by Fe-doping in the B2-type lattice (chemical disorder in the B- and D-lattices reduces the odd line intensity) and (ii) the reflection peak width varies for different Fe-doped samples. This variation can be, in principle, attributed mainly to crystalline grain size (d), which can be estimated using Scherrer formula (Table 1). d-Values in Table 1 are associated with the inverse of line broad-

Table 1
Parameters obtained from the analysis of the X-ray patterns (grain size – d; lattice parameter – a) and magnetization data (magnetization step-like variation – $\Delta M/M_A = [(M_A - M_M)/M_A]$, where M_A and M_M are respectively the maximum and minimum magnetization values of the A and M states, T_M is the martensitic temperature and $T_C{}^A$ is the austenitic magnetic ordering temperature).

Alloy	(a ±0.004) (Å)	(d ±2) (nm)	$\Delta M/M_A$ (%)	(T_M ±2) (K)	($T_C{}^A$ ±3) (K)
1% ^{57}Fe–Ni	6.005	15	36	195	325
1% ^{57}Fe–Mn	6.010	14	37	223	327
1% ^{57}Fe–Sn	6.004	20	49	254	323
0% ^{57}Fe	6.005	24	48	220	325

ening of a specific Bragg peak, allowing to estimate the size in that specific crystallographic direction (it was taken the most intense Bragg (2 2 0) peak to estimate the crystalline grain size).

Therefore, as shown in Table 1, the samples have distinct d-values, which may influence their magnetic properties, as it will be shown later on. It must be also mentioned that the lattice parameter (a) of the $L2_1$-type structure is constant within the error for the different samples, suggesting that the Fe-doping procedure is not drastically affecting the $L2_1$-structure cell volume. In resume, from X-ray analysis, it can be inferred that Fe-substitution in different lattice sites of the $Ni_{50}Mn_{36}Sn_{14}$ Heusler-type alloy leads first the $L2_1$-B2-type structure formation and this structure has an additional chemical disorder due to the Fe-doping. Therefore, in this article, it will be shown in more details how chemical disorder affects the structural phase transition (MPT) and related magnetic properties.

The FC- and FH-$M(T)$ curves of the as-annealed samples are displayed in Fig. 2(b). The main parameters discussed in this work are defined relatively to the Fe un-doped sample (0% Fe), taken as the reference sample. It should be first noted that, for all cases, the MPT temperature is different whether cooling or heating the samples. Consequently, this transformation is labeled according to the resulting phase: (i) A, for the austenitic phase and (ii) M, for the martensitic phase. The transition extends over a relatively broad range of temperature; the MPT typically begins at temperature T_{Ms} (or T_{As}) going up to T_{Mf} (or T_{Af}) temperatures. As indicated by arrows in Fig. 2(b), initial and final martensitic (T_{Ms}, T_{Mf}) and austenitic (T_{As}, T_{Af}) temperatures are respectively defined from FC and FH curves. To better characterize the magnetization step-like variation at the martensitic transition, an additional parameter is defined as: $\Delta M/M_A = [(M_A - M_M)/M_A]$, where M_A and M_M are the maximum and minimum magnetization values, respectively, of A and M states. The Curie temperature of the A phase (T_C^A) was estimated from the inflection point of the $M(T)$ curves recorded in a Faraday balance with a probe field of about 500 Oe. The T_C^A value is independent of the Fe-doping in the different samples, suggesting that the predominant ferromagnetic interactions among the Mn atoms in the $L2_1$-structure (on the B-lattices) are not severely modified by the Fe-substitution.

At the MPT temperature region, Fig. 2(b) displays changes in the FC- and FH-$M(T)$ curves, depending on what constituent elements Fe atoms are replacing in the alloy. Particularly, the 1% ^{57}Fe–Sn $M(T)$ curves display a sharp magnetization change at the MPT region, whereas a broad magnetization variation is observed in other Fe-doped samples. This broad MPT suggests a distribution of T_M-values caused either by Mn-chemical disorder or by some stoichiometric variation (T_M is strongly dependent on the excess of Mn in the $Ni_{50}Mn_{50-x}Sn_x$ alloys with $L2_1$-B2-type structure [4,6]). Additionally, one also notes that: (i) T_M-values are relatively different, depending on the Fe-lattice site occupations and (ii) the $\Delta M/M_A$ parameter (Table 1) is intrinsically correlated to modifications in the Mn-neighborhood and the grains size (d).

The influence of chemical disordering on the magnetism and on the MPT of the $Ni_{50}Mn_{36}Sn_{14}$ Heusler-type alloy have been investigated locally by performing RT ($L2_1$-type structure) Mössbauer spectroscopy at ^{57}Fe as well as at ^{119n}Sn nucleus-probes. The RT ^{57}Fe (a) and ^{119n}Sn (b) spectra of the Fe-doped samples are presented in Fig. 3 panels. ^{119n}Sn spectrum of the Fe un-doped sample (0% Fe) (not shown) is similar to that for the 1% ^{57}Fe–Mn sample displayed in Fig. 3(b).

The RT spectra shown in Fig. 3(a) and (b) have two broad components, except in the case of the ^{57}Fe spectrum for the 1% ^{57}Fe–Sn sample, in which only a single broad absorption line is observed. The fittings of these ^{57}Fe and ^{119n}Sn spectra were performed with two subspectra: a distribution of hyperfine magnetic fields (fraction f_{FM}) and a broad singlet (fraction f_{PM}). The line broadening effect

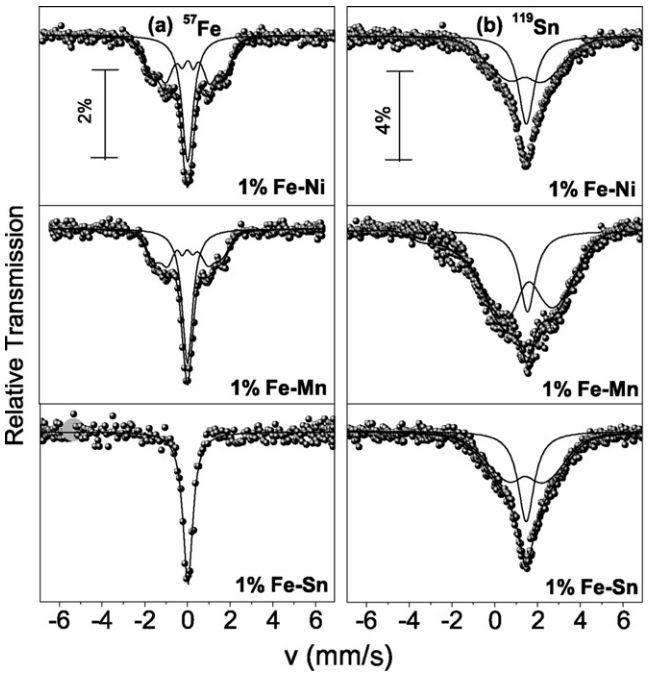

Fig. 3. Room temperature ^{57}Fe (a) and ^{119}Sn (b) Mössbauer spectra of the 1% Fe–X (X = Ni, Mn and Sn) alloys. The ^{57}Fe spectra were obtained with 512 channels whereas the ^{119}Sn were taken with 1024. The two subspectra used to fit the spectra are also shown: a singlet and a magnetic hyperfine field components.

and also the different f_{FM} and f_{PM} fractions in different samples support the fact that both Sn and Fe are distributed in non-equivalent chemical sites. The hyperfine parameters obtained from these fittings are presented in Table 2.

In the ordered $Ni_{50}Mn_{25}Sn_{25}$ Heusler alloy, only a well-resolved sextet is observed in the ^{119}Sn spectrum at RT [28]. The physical origin of this sextet is attributed to the transferred magnetic hyperfine fields from Mn atoms ferromagnetically coupled in B-sites. In our case, due to Mn excess occupying D-sites originally for Sn, the ^{119}Sn-spectra display two components as mentioned above. Therefore, the singlet, observed at ^{119}Sn-sites ($^{Sn}f_{PM}$), can be attributed to ^{119}Sn atoms with no transferred magnetic hyperfine fields (B_{hf}^{Tr}). Then, the possible chemical environments of these ^{119}Sn atoms in the $L2_1$-B2-type structure may be due neighborhood of Mn atoms in D-sites having either negligible magnetic moment [2–4] and/or in a disordered magnetically state (Ni and Sn atoms are in their respective sites). Consequently, the observed Sn MHFD component ($^{Sn}f_{FM}$) can be associated with ^{119}Sn atoms in regions at D-sites with non zero B_{hf}^{Tr}, i.e., close to Mn–Mn atoms ferromagnetically coupled. On the other hand, ^{57}Fe atoms also show complex magnetism from the Mössbauer point of view. The singlet subspectrum (fraction $^{Fe}f_{PM}$) of the Fe-doped samples can be attributed to Fe atoms either in Ni (A and C) or in Sn (D) lattice sites. In the Ni-sites, Fe atoms will have negligible magnetic moments, whereas in Sn-sites the substituted Fe atoms keep some magnetic moments. The later favors AF coupling with Mn-atoms in B-sites and orders magnetically below 90 K, consistent with the exchange bias effect observed below this temperature [23]. Low temperature Mössbauer spectrum (not shown) displays magnetic ordering for the singlet component, leading us to associate the singlet with Fe-atoms in paramagnetic state at RT. The MHFD component ($^{Fe}f_{FM}$) can be attributed to Fe atoms in the B-lattice sites, having FM interactions preferentially with Mn atoms (B-lattice sites of the $L2_1$-structure). Therefore, Mössbauer data show dependent T_M-value with the $^{Fe}f_{FM}$ fraction, as presented in Tables 1 (T_M) and 2 ($^{Fe}f_{FM}$). In general, these results indicate that the

Table 2
Hyperfine parameters [average magnetic hyperfine field[a] (B_{hf}), isomer shift[b] (δ), and relative absorption areas for the magnetic (f_{FM}) and paramagnetic (f_{PM}) components] obtained from the fittings of the RT ^{119}Sn and ^{57}Fe Mössbauer spectra of the Fe-doped samples (1% ^{57}Fe–X, X = Ni, Mn and Sn). The ^{57}Fe δ values are given relative to the metallic α-Fe value recorded at RT. The ^{119}Sn δ values are relatively to the source[a].

Mössbauer from ^{57}Fe (T = 298 K)			
MHFD ($^{Fe}f_{FM}$)	1% ^{57}Fe–Ni Area (%): 60 B_{hf} (T): 11 δ (mm/s): 0.15	1% ^{57}Fe–Mn Area (%): 51 B_{hf} (T): 10 δ (mm/s): 0.14	1% ^{57}Fe–Sn –
Singlet ($^{Fe}f_{PM}$)	Area (%): 40 δ (mm/s): 0.15	Area (%): 49 δ (mm/s): 0.14	Area (%): 100 δ (mm/s): 0.14
Mössbauer from ^{119}Sn (T = 298 K)			
MHFD ($^{Sn}f_{FM}$)	1% ^{57}Fe–Ni Area (%): 63 B_{hf} (T): 1.5 δ (mm/s): 1.41	1% ^{57}Fe–Mn Area (%): 85 B_{hf} (T): 2.2 δ (mm/s): 1.57	1% ^{57}Fe–Sn Area (%): 65 B_{hf} (T): 2.0 δ (mm/s): 1.42
Singlet ($^{Sn}f_{PM}$)	Area (%): 37 δ (mm/s): 1.48	Area (%): 15 δ (mm/s): 1.53	Area (%): 35 δ (mm/s): 1.47

[a] Uncertainty of B_{hf}: $\Delta B_{hf} = \pm 1$ T for ^{57}Fe and $\Delta B_{hf} = \pm 0.3$ T for ^{119}Sn.

[b] Uncertainty of δ: $\Delta\delta = \pm 0.02$ mm/s.

increase of the $^{Fe}f_{FM}$ fraction in the alloy will result in a reduction of T_M-values.

From these Mössbauer data, it can be concluded that not all Fe atoms occupy the nominal lattice sites in the $L2_1$-B2-type structure just by a simple chemical replacement procedure. The different fractions and the absorption resonant line broadening for both Fe and Sn environments are thought to be due to a chemical disordering effect both in B- and D-lattice sites of the $Ni_{50}Mn_{36}Sn_{14}$ Heusler-type alloy. Fe-substitutions occur preferentially on the B-lattices (FM fraction) in case of Fe–Ni and Fe–Mn doped samples, whereas the Fe preferential occupation in D-lattice sites occurs for the Fe–Sn case. Therefore, the different fractions $^{Fe}f_{FM}$ and $^{Fe}f_{PM}$ for the Fe–Ni and the Fe–Sn doped samples are responsible for their different T_M-values. In other words, larger T_M-value in Fe–Sn doped sample than in Fe–Ni sample can be associated with the larger AF contribution in the former ($^{Fe}f_{PM}$ that orders below 90 K), as reported in the literature for the Ni–Mn Heusler-based alloys [5,6]. In addition, our data clearly show a relation between the $^{Fe}f_{FM}$ fraction and the martensitic transition temperature T_M, as shown in Fig. 4 (it demonstrates that as higher is the $^{Fe}f_{FM}$ fraction lower

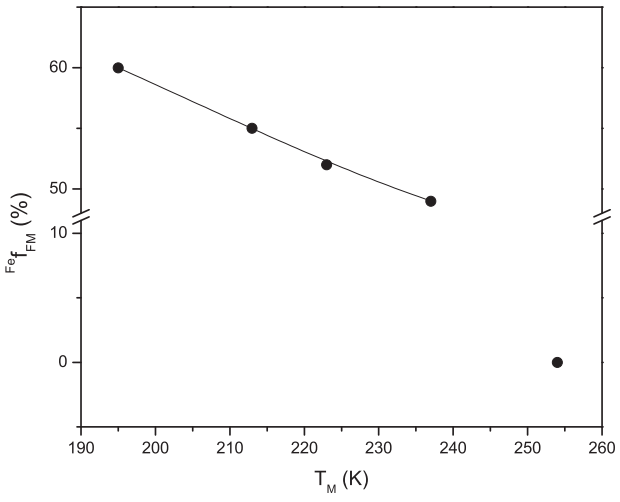

Fig. 4. Behavior of $^{Fe}f_{FM}$ (FM fraction obtained from ^{57}Fe Mössbauer spectra) against T_M (martensitic transition temperature) for the $Ni_2Mn_{1.44}Sn_{0.56}$ Heusler-type alloy of this work. The data are from Tables 1–3. The line connecting the experimental data is a guide for eyes.

should be the T_M-value). This result indirectly suggests that if the $Ni_2Mn_{2-x}Sn_x$ Heusler-type alloys are strongly FM no MPT occurs and for a fix Sn-content, the T_M value will depend on the intrinsic chemical order responsible for the AF (or FM) couplings, as recently reported for the Ni_2MnAl Heusler alloy [25].

Apart from the chemical disordering effect enhanced by the Fe-substitution process, it is known that the $Ni_{50}Mn_{50-x}Sn_x$ Heusler-type alloys are materials mechanically fragile and can be easily powdered [6]. This feature may limit its technological application. In order to study how grain size and chemical disorder influences of the magnetic properties of the alloy, it was prepared a new set of samples of 2 g-button containing about 1% ^{57}Fe replacing Ni, Mn or Sn (1% ^{57}Fe–X, X = Ni, Mn, Sn). In this paper, we present particularly the results of the 1% ^{57}Fe–Mn sample, because the others are similar.

In general, the buttons were firstly grounded by high energy milling process aiming to reduce grain size and to enhance of chemical disordering. Secondly, parts of the milled powders were heat-treated in an attempt to restore the initial crystallographic and chemical states. Fig. 5 displays the results of the X-ray (a), magnetization (b) and ^{57}Fe Mossbauer spectroscopy (c) obtained for the 1% ^{57}Fe–Mn sample in the following conditions: un-milled (called as NM), milled for 220 s (labeled M-220s) and milled for 220 s and 1 h-annealing at 1123 K (labeled as MHT-220s).

From the X-ray point of view, it can be observed that the milling process causes disappearance of the (1 1 1) reflection peak for the M-220s sample, reflecting an enhancement of the chemical disorder. All reflection peaks are much broader for the milled sample (M-220s) comparatively to those for the un-milled one. Thus, we estimated d-values (assuming line broadening due to grain size reduction) to be 26 nm for NM and 8 nm for NN-220s sample. Concomitantly, the parameters related to the MPT and the magnetic properties (for example, magnetization) were also found to change severely after milling, as can be seen in Table 3. On the other hand, it is observed that the sample MHT-220s has the d- and $\Delta M/M_A$-parameters recovered when compared with those of the un-milled sample, but the cubic lattice parameter a, M_M^{70K} (magnetization at 70 K in M state) and T_M values decreased, suggesting a reduction of crystal strain/defects when compared with the un-milled sample.

Specifically, the magnetization values in A and M states substantially reduce for the milled sample, suggesting that the chemical disorder produces regions in the sample with low Mn magnetic moments. Since the milling process leads the material to a nanocrystalline state, it is known from the literature that many

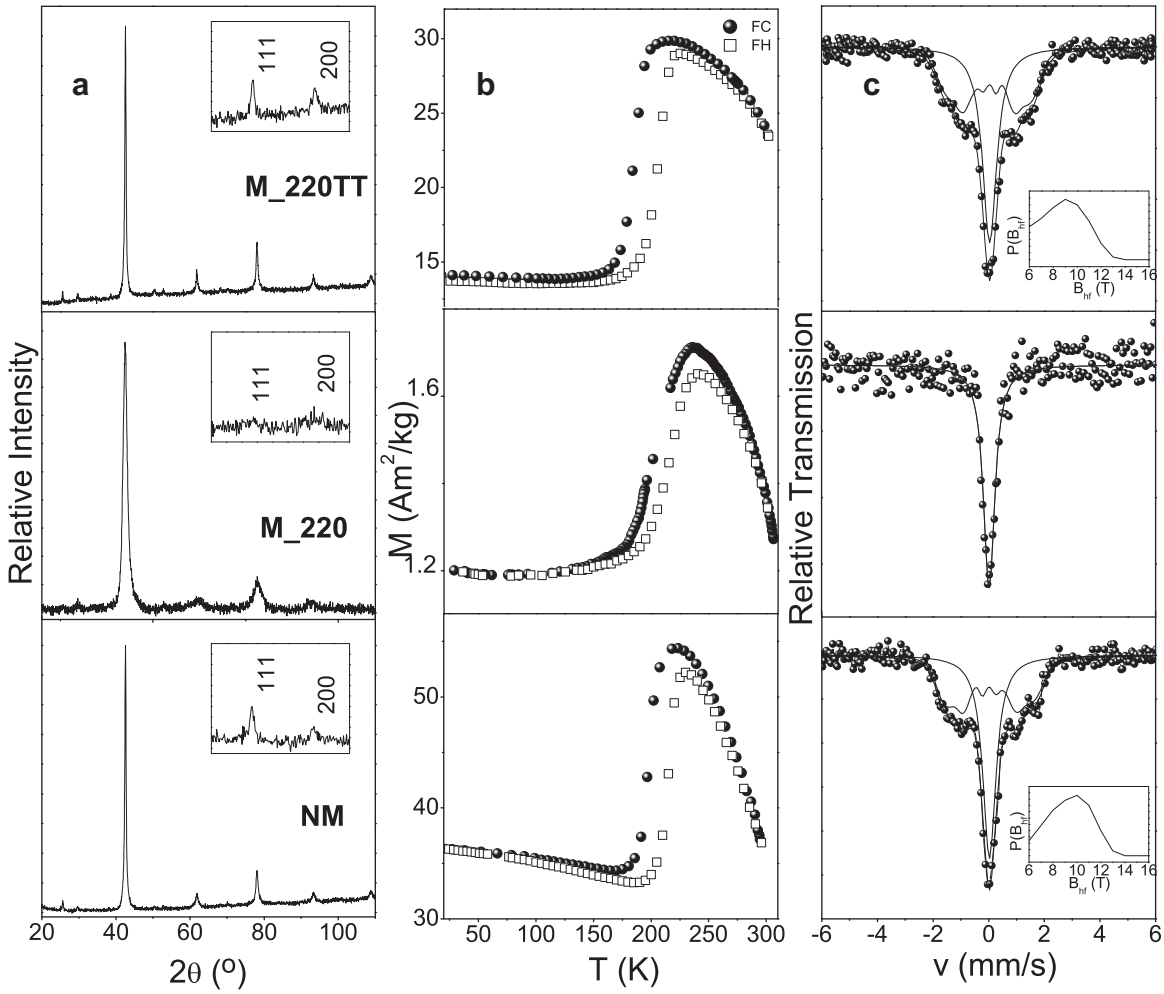

Fig. 5. (a) X-ray patterns, (b) FC and FH $M(T)$ curves and (c) ^{57}Fe Mössbauer spectra for the $Ni_{50}Mn_{35}{}^{57}FeSn_{14}$ Heusler-type alloy (NM), milled for 220 s (M-220s) and milled and annealed at 1023 K for one hour (MHT-220s).

properties can be described in terms of a core-shell model, where the grain core keeps the bulk magnetic properties of the crystalline materials and the shell is usually assumed to be topological and magnetically disordered due to the symmetry break in the grain boundary [27]. Thus, assuming a core-shell model, the reduction of magnetization-value is understandable taking into account an increase of the grain boundary volume, and consequently, an increasing of the Mn atoms fraction, in this region. Therefore, the core is responsible for the behavior of the $T_C{}^A$, T_M and $\Delta M/M_A$, whereas the shell contributes with frustrated magnetic interactions. The later is supported by the fact that the recorded $M(H)$ curves (not shown) do not reach saturation regime for applied field of 3 T in case of milled samples. After the heat treatment, the grain size (d) is increased to 31 nm and, concurrently, the $\Delta M/M_A$ has its value recovered to the NM state. Therefore, the heat-treated sample recovers the $^{Fe}f_{FM}$ fraction and indicates that $T_C{}^A$, T_M and $\Delta M/M_A$ are intrinsically related to the ordered fraction of the sample. Additionally, ^{57}Fe Mössbauer spectra clearly show that the milling procedure induces an increasing of the singlet component, which may be assigned to Fe in Mn–Mn frustrated magnetic state in the grain boundary as well as in the core (chemical disorder) regions. The M-220s sample seems to still have a fraction of the MHFD component (dispersed in the spectrum background) since it is sensed by magnetization data (presence of the MPT).

In summary, it was found that the enhancement of the chemical disordering induced by Fe-doping process is different from that obtained by reducing the grain size of the sample by milling. In the former case, the Fe-substitution effect modifies the magnetic properties basically due to elemental occupation on different lattice sites of the $L2_1$-type structure (producing different FM and AF fractions). On the other hand, the milling process yields a grain size reduction that favors the volume fraction enhancement of the shell regions, which have frustrated magnetic states. In both cases, the FM fraction (MHFD component) governs $T_C{}^A$, T_M and $\Delta M/M_A$

Table 3
Parameters obtained from the analysis of the X-ray patterns (grain size – d; lattice parameter – a); magnetization data [magnetization at 70 K in M state ($M_M{}^{70K}$), magnetization step-like variation – $\Delta M/M_A = [(M_A - M_M)/M_A]$, where M_A and M_M are respectively the maximum and minimum magnetization values of the A and M states, martensitic temperature (T_M) and austenitic magnetic ordering temperature – $T_C{}^A$] and ^{57}Fe Mössbauer spectroscopy ($^{Fe}f_{FM}$ – fraction of Fe atoms in magnetically ordered state at 300 K).

Process	(a ±0.004) (Å)	(d ±2) (nm)	($M_M{}^{70K}$ ±0.1) (Am²/kg)	$\Delta M/M_A$ (%)	(T_M ±2) (K)	($T_C{}^A$ ±3) (K)	$^{Fe}f_{FM}$ (%)
MHT-220s	5.815	31	14.0	51	213	328	55
M-220s	6.003	8	1.2	26	233	326	0
NM	6.010	26	36.3	54	237	323	49

values. The latter is the most important parameter responding for the giant magnetocaloric effect of the $Ni_{50}Mn_{36}Sn_{14}$ Heusler-type alloy, consequently a quantity that deserves to be better understood and controlled in this potentially magnetic refrigerant material.

4. Conclusion

Annealed $Ni_{50}Mn_{36}Sn_{14}$ Heusler-type alloy with elemental replacement corresponding to 1 at.% of Fe in Ni, Mn or Sn lattice sites of the $L2_1$-structure was systematically studied with X-ray diffraction (XRD), Mössbauer spectroscopy and magnetometry. It was also investigated the chemical disorder induced by high energy ball milling process with these techniques. XRD patterns reveal that the $L2_1$-B2-type structure increases its chemical disorder due to different atomic arrangements on the $L2_1$-type occupation of lattice sites in the Fe-doped samples. The milling process also induces an enhancement of the chemical disorder as shown by the absence of the (1 1 1) reflection peak for the milled sample. From Mössbauer point of view, it was found that Fe atoms occupy partially the B-lattice sites for Fe–Ni and Fe–Mn samples, whereas they preferentially occupy D-lattice sites for the Fe–Sn sample. In addition, the line broadening effect and also the different ferromagnetic (f_{FM}) and paramagnetic (f_{PM}) fractions at room temperature in different samples support the argument that both Sn and Fe are distributed in non-equivalent chemical sites. It was also found that: (i) the martensitic transition temperature is intrinsically related to the fraction of Fe atoms ferromagnetically coupled with Mn (Fe atoms in B lattice sites) in the $L2_1$-B2-type structure, i.e., large FM fraction lead to a low T_M-value and (ii) the ferromagnetic interactions are reduced either by the Fe-substitution effect or by milling due to the increasing chemical disorder. Moreover, milled samples can be analyzed assuming the core-shell model, where one has considered that the fraction of atoms in the shell (grain boundary regions) increases after the milling. Therefore, the chemical disorder is enhanced and there is a substantial reduction of crystalline grain size. These two effects respond for reducing the alloy net magnetization as well as the magnetization variation ($\Delta M/M_A$) associated with the martensitic phase transformation in the $M(T)$ curves. Particularly, the decreasing of the $\Delta M/M_A$ value in the milled compared to the un-milled samples represents a significant reduction of the magnetocaloric property of this alloy. Finally, it should be important to mention that: (i) the $L2_1$-B2-type structure can be recovered after annealing, for short times of heat treatment, the milled samples and (ii) Fe-substitution for other elements, namely Ni, Mn or Sn, in this alloy makes it possible to extend the milling process to approximately 220 s, preserving the martensitic phase transformation. This result, which was observed for these three Fe-doped samples, is different from that observed for the un-doped sample, for which a phase segregation effect was always observed for milling times as long as than 90 s.

Acknowledgments

The authors would like to thank CAPES, FINEP, FAPES, CNPq/MCT and UFES for the financial support and also the Arcelor/CST for supplying us with liquid nitrogen.

References

[1] D.P. Morris, C.D. Price, J.L. Hughes, Acta Cryst. 16 (1963) 839.
[2] A. Ayuela, J. Enkovaara, K. Ullakko, R.M. Nieminen, J. Phys. Condens. Matter 11 (1999) 2017.
[3] H.E. Şaşıoğlu, First-principles study of the exchange interactions and curie temperature in Heusler alloys, Doctoral Thesis, Mathematisch –Naturwissens chaftlich – Technischen Fakultät der Martin – Luther – Universität Halle, Wittenberg, 1975.
[4] R.B. Helmholtz, K.H.J. Buschow, J. Less Comm. Met. 128 (1987) 167.
[5] T. Krenke, E. Duman, M. Acet, E.F. Wassermann, X. Moya, L. Mañosa, A. Planes, Nat. Mater. 4 (2005) 450.
[6] T. Krenke, M. Acet, E.F. Wassermann, X. Moya, L. Mañosa, A. Planes, Phys. Rev. B 72 (2005) 014412.
[7] K. Otsuka, C.M. Wayman (Eds.), Shape Memory Materials, Cambridge University Press, 1998.
[8] I. Galanakis, E. Şaşıoğlu, K. Özdoğan, Phys. Rev. B 77 (2008) 214417.
[9] J. Marcos, L. Mañosa, A. Planes, F. Casanova, X. Batlle, A. Labarta, Phys. Rev. B 68 (2003) 094401.
[10] T. Krenke, E. Duman, M. Acet, X. Moya, L. Mañosa, A. Planes, J. Appl. Phys. 102 (2007) 033903.
[11] R. Kainuma, K. Oikawa, W. Ito, Y. Sutou, T. Kanomata, K. Ishida, J. Mater. Chem. 18 (2008) 1837.
[12] P.J. Webster, K.R.A. Ziebeck, S.L. Town, M.S. Peak, Philos. Mag. B 49 (1984) 295.
[13] E. Şaşıoğlu, L.M. Sandratskii, P. Bruno, Phys. Rev. B 77 (2008) 064417.
[14] K. Koyama, T. Kanomata, R. Kainuma, K. Oikawa, K. Ishida, K. Watanabe, Physica B 383 (2006) 24.
[15] P.J. Brown, A.P. Gandy, K. Ishida, R. Kainuma, T. Kanomata, K.-U. Neumann, K. Oikawa, B. Ouladdiaf, K.R.A. Ziebeck, J. Phys. Condens. Matter 18 (2006) 2249.
[16] Y. Sutou, Y. Imano, N. Koeda, T. Omori, R. Kainuma, K. Ishida, K. Oikawa, Appl. Phys. Lett. 85 (2004) 4358.
[17] R. Kainuma, Y. Imano, W. Ito, H. Morito, Y. Sutou, K. Oikawa, A. Fujita, K. Ishida, S. Okamoto, O. Kitakami, T. Kanomata, Appl. Phys. Lett. 88 (2006) 192513.
[18] K. Ullakko, J.K. Huang, C. Kantner, R.C. O'Handley, V.V. Kokorin, Appl. Phys. Lett. 69 (1996) 1966.
[19] S. Aksoy, T. Krenke, M. Acet, E.F. Wassermann, X. Moya, L. Mañosa, A. Planes, Appl. Phys. Lett. 91 (2007) 251915.
[20] E.C. Passamani, F. Xavier, E. Favre-Nicolin, C. Larica, A.Y. Takeuchi, I.L. Castro, J.R. Proveti, J. Appl. Phys. 105 (2009) 033919.
[21] E.C. Passamani, C. Córdova, A.L. Alves, P.S. Moscon, C. Larica, A.Y. Takeuchi, A. Biondo, J. Phys. D Appl. Phys. 42 (2009) 215006.
[22] S. Chatterjee, S. Giri, S.K. De, S. Majumdar, Phys. Rev. B 79 (2009) 092410.
[23] A.L. Alves, E.C. Passamani, V.P. Nascimento, A.Y. Takeuchi, C. Larica, J. Phys. D Appl. Phys. 43 (2010) 345001.
[24] S. Askoy, M. Acet, P.P. Deen, L. Mañosa, A. Planes, Phys. Rev. B 79 (2009) 212401.
[25] I. Galanakis, E. Şaşıoğlu, Appl. Phys. Lett. 98 (2011) 102514.
[26] M. Pugaczoa-Michalska, A. Jezierski, J. Dubowik, J. Kaczkowski, Acta Phys. Pol. A 115 (2009) 241.
[27] E.C. Passamani, B.R. Segatto, C. Larica, R. Cohen, J.M. Greneche, J. Magn. Magn. Mater. 322 (2010) 3917.
[28] L. Cäer, E.A. Leonocva, P. Delcroix, S.D. Kaloshkin, Y.V. Baldokhin, J. Metast. Nanocryst. Mater. 15 (2002) 239.